

The influence of electric fields on nanostructures—Simulation and control

Frank Haußer^a, Sandra Rasche^b, Axel Voigt^{b,*}

^a *Fachbereich II Mathematik, Technische Fachhochschule Berlin, Luxemburger Straße 10, 13353 Berlin, Germany*

^b *Institut für Wissenschaftliches Rechnen, Technische Universität Dresden, Zellescher Weg 12-14, 01062 Dresden, Germany*

Received 23 February 2009; received in revised form 14 May 2009; accepted 25 May 2009

Available online 23 June 2009

Abstract

Macroscopic electric fields may be used to influence or even control the shape evolution of single layer islands on a crystalline surface. We validate a phase-field approach to simulate such shape evolutions by comparison with simulations based on a sharp interface approach. The phase-field model is then used to formulate and discretize the control problem of finding an electric field which drives an island to a predefined shape. Some first results of this approach are presented.

© 2009 IMACS. Published by Elsevier B.V. All rights reserved.

Keywords: Optimal control of free boundary problems; Cahn–Hilliard equation; Adaptive finite elements; Electromigration; Surface evolution

1. Introduction

The manipulation of nanostructures by macroscopic forces is likely to become a key ingredient in many nanotechnology applications. Understanding the influence of external fields on the shape evolution of nanoscale surface features is therefore of considerable importance. Electric fields, for example, have become one of the most widely used tools for manipulating cells, biomolecules and nanoparticles in microfluidic devices [12]. In this article we are interested in the effects of an electric current (driven by an electric field) on single-layer (i.e. atomic height) islands on a crystalline surface and in the possibility to use these effects to manipulate and control the shape evolution of the nanoscale islands. The island evolves under surface electromigration, the directed motion of adsorbed atoms (adatoms) due to the slight force transmitted by collisions with the conduction electrons in the sample. Electromigration along interfaces and grain boundaries is the most persistent and menacing reliability problem in integrated circuit technology [20]. Correspondingly, much work has been devoted to electromigration induced void formation and breakdown in metallic conductor lines, and the capacity for quantitative numerical modeling has been demonstrated at least for simple void geometries [5,18,3,2]. A major obstacle to achieving predictive power in such studies, however, is the insufficient control over the complex internal structure of the polycrystalline samples. Hence an important motivation for investigating electromigration induced effects on simple, well-controlled nanoscale morphologies, such as single-layer island (see Fig. 1), is to bridge the gap between the microscopic mechanisms of electromigration and their consequences on

* Corresponding author.

E-mail address: axel.voigt@tu-dresden.de (A. Voigt).

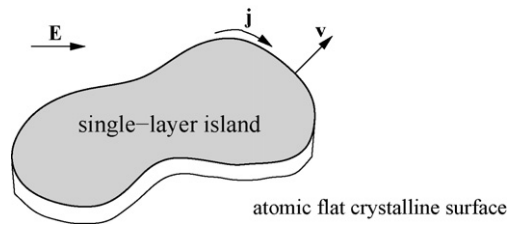


Fig. 1. Sketch of a single-layer (atomic height) island on a crystalline, atomic flat surface.

technologically relevant length and time scales. Electromigration of islands has been modeled previously using Monte Carlo simulations [14,17] and continuum theory [16,11,6].

Here we focus on the regime of periphery diffusion, where the dominant kinetic process is the migration of atoms along the island boundary. The shape then follows a local evolution law, without coupling to the adatoms diffusing on the surrounding crystalline surface. Assuming isotropic line energy of the island boundary and isotropic mobility of atoms moving along the boundary, the local normal velocity v satisfies a continuity equation, which in non-dimensional form reads (see Fig. 1)

$$v = -\partial_s j, \quad j = -\partial_s \kappa + E_t. \quad (1)$$

Here κ denotes the curvature of the island boundary, E_t the tangential component of the local electric field (= electromigration force) and s the arclength along the island boundary. Thus, the total mass flux j along the island boundary is driven by the tangential derivative of the chemical potential $\mu = \kappa$ (1d-surface diffusion) and the electromigration force E_t . For later use we recall, that in the continuum setting the chemical potential μ is obtained as the functional derivative of the line energy with respect to normal variations. Also note that Eq. (1) implies, that the island evolution preserves the area of the island: movement and shape change of the island happens via the transport of island atoms along the boundary. Since the tangential electric field may be expressed in terms of an electric potential U_{el} as $E_t = -\partial_s U_{el}$, Eq. (1) may equivalently be written as

$$v = \partial_{ss}(\kappa + U_{el}). \quad (2)$$

For atomic layer height islands on a thick sample, the island boundary has a negligible effect on the electric field. Therefore Eq. (1) is a purely local geometric evolution equation with a predefined external field E , which may assumed to be constant in space. The richness of the dynamical behaviour of this model and of its anisotropic generalization has been investigated in [10] and [11], which leads us to believe that microscopic island shapes are able to be controlled through a macroscopic electric field. Applied to real systems, this could have a large technological impact, for example in designing novel electronic devices.

In this work we will restrict to the isotropic case and consider the following scenario:

Problem. Given an island shape and position at time $t = 0$, and some desired shape and position at time $t = T$, find a suitable external electric field $E = E(t)$ (constant in space, but changing in time) such that the evolution of the initial island according to Eq. (1) leads to the desired shape and position.

This is in fact an optimal control problem of a free boundary problem, where the free boundary is the island boundary and the control variable is the electric field E .

To formulate the control problem we first present a diffuse-interface approximation of Eq. (1) in Section 2 and discuss a discretization using adaptive finite elements. Subsequently we validate the diffuse-interface approximation by comparing some simulation results with results obtained with a discretization of the sharp-interface formulation (1). In Section 3 we formulate the optimal control problem based on the diffuse-interface formulation. After introducing a suitable cost functional, the formal Lagrangian framework is utilized to derive the first-order necessary optimality conditions leading to a system of adjoint equations and a variational inequality. We present our numerical scheme for solving the adjoint equations. For the variational inequality, a simple gradient method is used. Finally we give some first results on controlled island evolution in Section 4 and draw some conclusions in Section 5.

2. Modeling

Instead of solving the geometric evolution equation directly, we will use a diffuse-interface approximation, with an order parameter ϕ distinguishing between two phases, namely the island – corresponding to regions where $\phi = 1$ – and the surrounding crystalline surface, where $\phi = 0$. Diffuse-interface or phase-field models are a fast growing area in computational materials science. It is a theory and computational tool for predictions of the evolution of arbitrarily shaped morphologies and complex microstructures. In the model the *diffuse* interface between two phases is treated as a region of finite thickness ε and the interface is represented implicitly through the level set $\phi = 0.5$. The time evolution of the order parameter, also called the phase-field, ϕ thus implicitly determines the evolution of the interface. A conservative evolution equation for the phase-field ϕ is obtained along the same lines as the sharp interface evolution Eq. (2) as a continuity equation for some flux J , which itself is driven by a chemical potential $\omega = \mu + U_{el}$:

$$\partial_t \phi = -\nabla \cdot J, \quad J = -\varepsilon^{-1} M(\phi) \nabla \omega.$$

Here the degenerate mobility $M(\phi) = 36\phi^2(1 - \phi)^2$ is responsible for restricting the diffusion to the diffuse-interface. Moreover, μ is obtained as the functional derivative of a Ginzburg–Landau free energy $F[\phi]$, the diffuse-interface counterpart of the line energy:

$$F[\phi] = \int_{\Omega} \frac{\varepsilon}{2} |\nabla \phi|^2 + \varepsilon^{-1} G(\phi) \, dx,$$

where Ω denotes the whole domain of the crystalline surface, and

$$G(\phi) = 18\phi^2(1 - \phi)^2$$

is a double well potential with minima at the two phases $\phi = 0$ and $\phi = 1$ and ε determines the width of the transition zone between the two phases $\phi = 0$ and $\phi = 1$. Introducing also a stabilizing function $g(\phi) = 30\phi^2(1 - \phi)^2$ (see [9]) one arrives at the following 4th order degenerate Cahn–Hilliard equation

$$\partial_t \phi = \varepsilon^{-1} \nabla \cdot (M(\phi) \nabla \omega) \tag{3}$$

$$g(\phi) \omega = -\varepsilon \Delta \phi + \varepsilon^{-1} G'(\phi) + U_{el}. \tag{4}$$

Note that for an electric field being constant in space, the electric potential U_{el} may be chosen as $U_{el} = -E(t) \cdot x$, $x \in \mathbb{R}^2$. For the case $U_{el} = 0$ and $g(\phi) = 0$, an asymptotic analysis $\varepsilon \rightarrow 0$ has been given in [4] showing the convergence towards the geometric evolution law Eq. (2). This result has been extended to the anisotropic case with the non-zero stabilization term in [15,13]. The incorporation of the electric field in the asymptotic analysis can be done along the same lines.

A major advantage of the diffuse-interface formulation compared with the sharp interface model is the possibility to easily handle topological changes. Furthermore it will be much more convenient to formulate the control problem in terms of the phase-field model, as will be shown in Section 3.

2.1. Discretization

To numerically solve the phase-field model we use periodic boundary conditions on a rectangular domain $\Omega \subset \mathbb{R}^2$ and initial condition $\phi(0) = \phi_0$. We will use a semi-implicit discretization in time, which results in a linear system to be solved in each time step. Therefore the derivative of the double well potential G is linearized by

$$G'(\phi^{n+1}) \approx G'(\phi^n) + G''(\phi^n)(\phi^{n+1} - \phi^n) = G''(\phi^n)\phi^{n+1} + G'(\phi^n) - G''(\phi^n)\phi^n,$$

with n denoting the discrete time instance. The semi-discrete formulation, with (\cdot, \cdot) denoting the L^2 scalar product on Ω reads

$$\left(\frac{\phi^{n+1} - \phi^n}{\tau}, \eta \right) = -\varepsilon^{-1} (M(\phi^n) \nabla \omega^{n+1}, \nabla \eta) \tag{5}$$

$$(g(\phi^n) \omega^{n+1}, \eta) = \varepsilon (\nabla \phi^{n+1}, \nabla \eta) + \varepsilon^{-1} (G''(\phi^n) \phi^{n+1}, \eta) + \varepsilon^{-1} (G'(\phi^n) - G''(\phi^n) \phi^n, \eta) + (U_{el}, \eta), \tag{6}$$

with appropriate test functions η and time steps $\tau = t^{n+1} - t^n$ for $n = 0, 1, 2, \dots$. Only the double-well potential is treated implicitly, whereas all other non-linear terms $M(\phi)$ and $g(\phi)$ are treated explicitly. We use linear finite elements

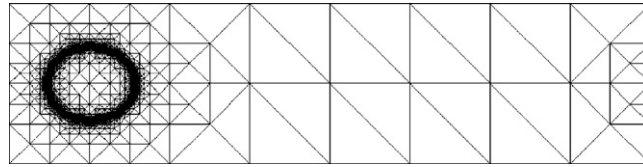


Fig. 2. Example for an adaptive mesh. The island radius is $r = 5$, and the initial configuration is shown. The local refinement on the right side results from the periodic boundary conditions. Compared with a global mesh the problem size could be reduced by at least two orders of magnitude.

for ϕ and ω to discretize in space. The resulting linear system is solved with a direct solver, which is possible due to the reduction in problem size by using adaptive mesh refinement and coarsening. The numerical scheme is implemented in the adaptive finite element toolbox AMDiS [21]. We use bisection to refine triangles according to an equidistribution strategy, which is based on an error estimator for the jump residual of $\partial_n \phi$ on element edges of the triangulation, which results in a fine resolution along the diffuse-interface and a coarse discretization away from it. In Fig. 2 an adaptively refined mesh for a typical situation is depicted.

2.2. Comparison with geometric evolution law

For a constant horizontal electric field $E = (1, 0)^T$, the island does move horizontally in the direction of the electric field and the shape of the island approaches different equilibrium shapes, depending on the size of the island. In the following examples, the initial shape is an ellipse with an aspect ratio close to one. Therefore, the different initial conditions will be labeled by the radius of the corresponding circle with the same area. Such a perturbed circle is chosen to reduce the computational time needed to achieve the equilibrium shape. We compare our results of the diffuse-interface model with numerical solutions of the geometric evolution Eq. (1). The latter is solved on the basis of parametric finite elements, see [1,7] for details. Fig. 3 (left) shows the evolution of an island with radius $r = 3.3$. The equilibrium shape remains close to a circle. This is no longer true for larger islands. Fig. 3 (right) shows the evolution for $r = 5$, which results in an elongated stationary shape. Further increasing the radius, leads to an instability and a pinch-off, resulting in a splitting of the island. Here the advantage of the diffuse-interface approximation is clearly seen, as the splitting cannot be handled directly within the sharp interface approach. Therefore the sharp interface simulation stops before the pinch-off occurs. In Fig. 4 the evolution for $r = 7$ is depicted. The numerical results confirm the results

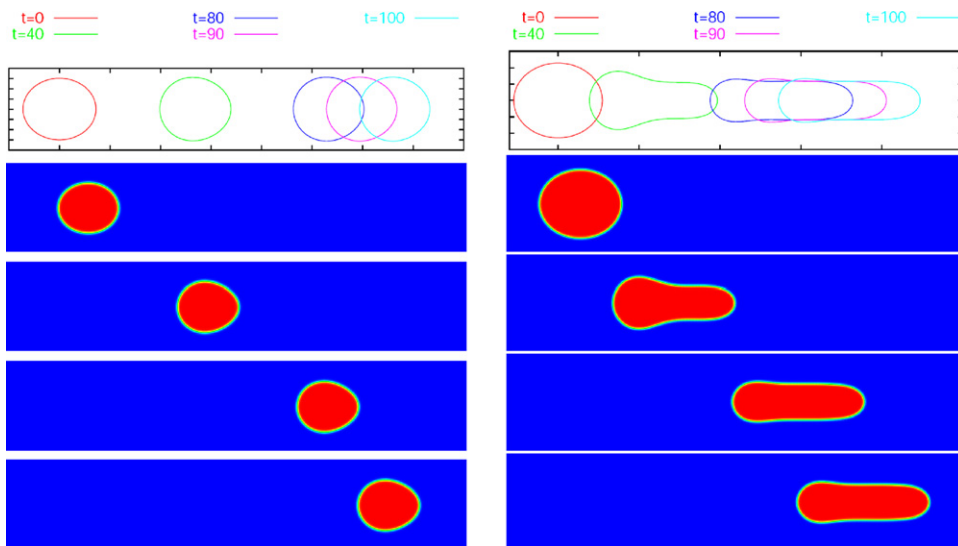


Fig. 3. Island evolution under the influence of a constant electric field $E = (1, 0)^T$. (Left column) initial configuration: ellipse with aspect ratio 1.2 and area πr^2 , $r = 3.3$. (Right column) initial configuration: ellipse with aspect ratio 1.2 and area πr^2 , $r = 5.0$. The uppermost row shows the sharp interface results for various timesteps. In the subsequent rows the phase-field simulations are shown for times $t = 0, 40, 80, 100$.

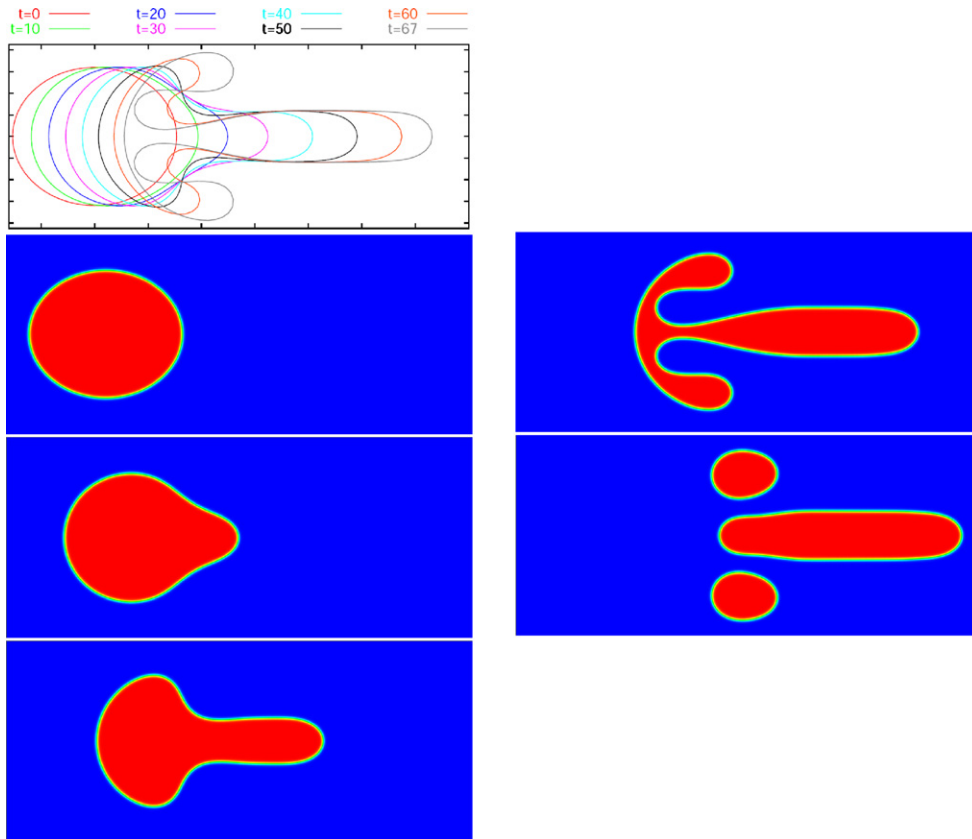


Fig. 4. Island evolution under the influence of a constant electric field $E = (1, 0)^T$. Initial configuration: ellipse with aspect ratio 1.2 and area πr^2 , $r = 7$; sharp interface results for various timesteps (top) and phase-field simulations for $t = 0, 20, 40, 60, 70$.

of the asymptotic analysis and allow us to use the diffuse-interface approximation for further studies on the control of island structures.

3. Control

3.1. Problem formulation

Instead of solving for the evolution of island shapes for a given electric field, we turn to the problem of finding an optimal electric field for a given island evolution. To be more precise, we specify an initial and a final shape and position of an island and want to find the corresponding electric field such that the initial island evolves in a given time as close as possible to the final shape. To formulate this as an optimal control problem, we define the following cost functional, which has to be minimized:

$$J(\phi, E) = \frac{1}{2} \int_{\Omega} (\phi(x, T) - \phi_e(x))^2 dx + \frac{\nu}{2} \int_0^T E \cdot E dt \tag{7}$$

with ϕ_e a phase-field function representing the desired shape and position of the island at time $t = T$ and $\nu > 0$ a penalty parameter. Thus, minimizing J corresponds to minimizing the L^2 distance of the island at $t = T$ from the desired shape (both encoded in the corresponding phase-field) and the average of the square of field strength.

Optimal control problem. Given an initial phase-field $\phi(\cdot, 0)$ at time $t = 0$ and a desired phasefield ϕ_e , find an electric field $E : [0, T] \rightarrow \mathbb{R}^2$ which minimizes the functional J given in (7), subject to the constraints given by the evolution

Eqs. (3) and (4) and the following box constraints on the electric field

$$E_{ad} = \{(E_1, E_2)^T, E_i \in L^2(0, T) : E_{\min} \leq E_i(t) \leq E_{\max}, \forall t \in [0, T]\}. \tag{8}$$

The problem is a parabolic optimal control problem of a free boundary, which is encoded through the phase-field variable. Theoretical results for this type of problems, especially for the control of phase-field problems can be found in [8,19]. However, these approaches have not been realized within a numerical scheme so far. In order to tackle the problem we use the Lagrange function to formulate the first-order optimality conditions. Introducing the Lagrange multipliers q_1 and q_2 (adjoint states) corresponding to the state Eqs. (3) and (4), respectively, the Lagrange function reads:

$$L(\phi, \omega, E, q_1, q_2) = J(\phi, E) - \int_0^T \int_{\Omega} (\partial_t \phi - \varepsilon^{-1} \nabla \cdot (M(\phi) \nabla \omega)) q_1 \, dx dt - \int_0^T \int_{\Omega} (g(\phi) \omega + \varepsilon \Delta \phi - \varepsilon^{-1} G'(\phi) - U_{el}) q_2 \, dx dt$$

with $U_{el}(t, x) = -E(t) \cdot x$. From this we formally obtain the necessary first-order optimality conditions for the optimal control \bar{E} with associated optimal states $\bar{\phi}, \bar{\omega}$ as

$$D_{\phi} L(\bar{\phi}, \bar{\omega}, \bar{E}, q_1, q_2) \phi = 0, \quad \forall \phi : \phi(0, x) = 0 \tag{9}$$

$$D_{\omega} L(\bar{\phi}, \bar{\omega}, \bar{E}, q_1, q_2) \omega = 0, \quad \forall \omega \tag{10}$$

$$D_E L(\bar{\phi}, \bar{\omega}, \bar{E}, q_1, q_2) (E - \bar{E}) \geq 0, \quad \forall E \in E_{ad}, \tag{11}$$

where D denotes the functional derivative. The evaluation of Eqs. (9) and (10) gives the system of adjoint equations

$$-\partial_t q_1 = -\varepsilon \Delta q_2 - \varepsilon^{-1} M'(\phi) \nabla \omega \cdot \nabla q_1 - g'(\phi) \omega q_2 + \varepsilon^{-1} G''(\phi) q_2 \tag{12}$$

$$g(\phi) q_2 = \varepsilon^{-1} \nabla \cdot (M(\phi) \nabla q_1), \tag{13}$$

which can be interpreted as a 4th order equation for q_1 . The system needs to be solved backwards in time with periodic boundary conditions and end condition $q_1(T) = \phi(T) - \phi_e$. Evaluating (11) yields the following variational inequality for the optimal control \bar{E} :

$$\int_0^T \left[\left(v \bar{E} - \int_{\Omega} x q_2 dx \right) \cdot (E - \bar{E}) \right] dt \geq 0, \quad \forall E \in E_{ad}. \tag{14}$$

We will follow the common approach to solve the first-order necessary conditions (and therefore the control problem, provided the conditions have also been sufficient) by utilizing the following optimization loop:

- (i) Solve the state Eqs. (3) and (4) forward in time using a given electric field.
- (ii) Solve the adjoint Eqs. (12) and (13) backward in time using the computed state variables obtained in (i).
- (iii) Update the electric field by utilizing the variational inequality (14) and proceed with step (i).

3.2. Discretization

As has been stated above, the state Eqs. (3) and (4) and the adjoint Eqs. (12) and (13) form a coupled system of non-linear partial differential equations in space-time. Thus, the solution of the adjoint system requires knowledge on the state variables at each time step. We solve the system by iteratively solving first the state equations forward in time, as described in Section 2 and then solving the adjoint equations backward in time, using the computed state variables. The semi-discrete weak formulation for the adjoint problem reads

$$\begin{aligned} \left(\frac{q_1^{n+1} - q_1^n}{\tau}, \eta \right) &= \varepsilon (\nabla q_2^n, \nabla \eta) - \varepsilon^{-1} (M'(\phi^n) \nabla \omega^n \nabla q_1^n, \eta) - (g'(\phi^n) \omega q_2^n, \eta) + \varepsilon^{-1} (G''(\phi^n) q_2^n, \eta) \\ (g(\phi^n) q_2^n, \eta) &= -\varepsilon^{-1} (M(\phi^n) \nabla q_1^n, \nabla \eta) \end{aligned}$$

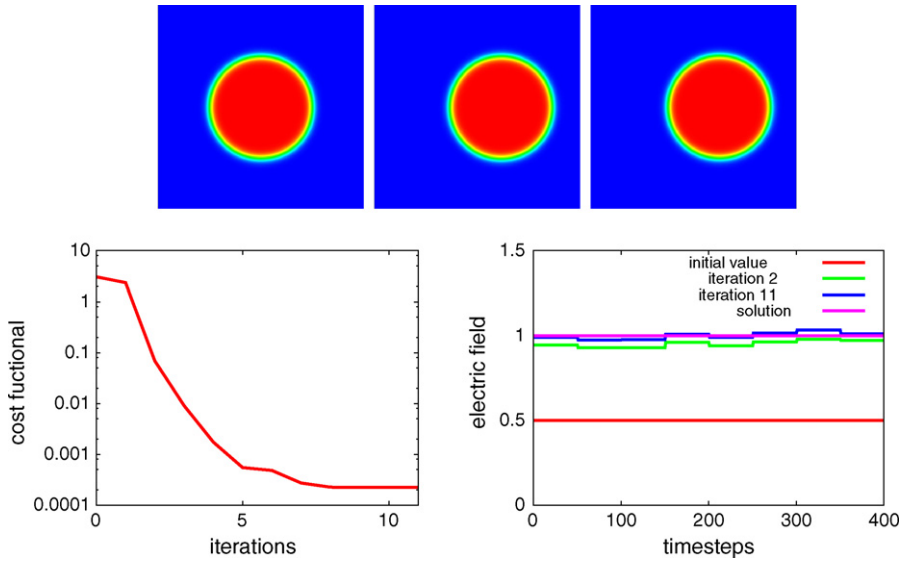


Fig. 5. Computed island position for a circular island with $r = 1.0$ at $t = T$ for iteration $k = 0, 2, 11$ (top row—from left to right). Cost functional in logarithmic scale (bottom left) and computed x -component of the electric field (bottom right) for iteration $k = 0, 2, 11$.

with appropriate test functions η . Note that here the unknowns are q_1^n, q_2^n and the system has to be solved for $n = N - 1, N - 2, N - 3, \dots$, with $t^N = T$. We use linear finite elements to discretize in space. The system is again implemented in AMDiS and the linear system is solved with a direct solver. For both the state and adjoint equations we now use a globally refined mesh to circumvent technical difficulties in the handling of different meshes for different components. An adaptive strategy will be discussed in a forthcoming paper.

Using a gradient method to update the electric field, the variational inequality (14) yields

$$E(t^n)^{(k+1)} = E(t^n)^{(k)} + \alpha^{(k)} \left(-\nu E(t^n)^{(k)} + \int_{\Omega} q_2^n x \, dx \right) \tag{15}$$

with k being the iteration number of the optimization loop and $\alpha^{(k)}$ a suitable chosen step size. As a simple strategy to regularize the gradient, we average the computed electric field over several time steps before it is used in the next forward simulation as input parameter. If necessary, the electric field is projected to the admissible range (8) by truncation.

4. Results

As a proof of concept we use some forward simulations as presented in Section 2 as test cases for the optimal control algorithm. We use the initial and end configuration of the simulation as ϕ_0 and ϕ_e , respectively but specify a different electric field as the initial guess $E(t^n)^{(0)}$. Fig. 5 shows the convergence of the electric field towards the desired constant value for a small island of $r = 1$. In this case the initial circular shape remains and the island only has to be moved from left to right. The reduction in the cost functional and the convergence of the electric field towards the constant value $E = (1, 0)^T$ is observed. A more complicated control problem is formulated for a larger island radius. Within a configuration where the stationary shape is an elongated island we again use initial and end configuration of a forward simulation with constant electric field to specify ϕ_0 and ϕ_e for the optimal control problem but use a different electric field as the initial guess $E(t^n)^{(0)}$. Fig. 6 shows the convergence of the electric field towards the desired constant value for a small island of $r = 3$. In addition to the movement of the island from left to right also the shape has to change. Also in this case the reduction in the cost functional and the convergence of the electric field towards the constant value $E = (2, 0)^T$ can be observed.

Both examples demonstrate the possibility to control the evolution of islands through variations in the electric field. For more complex situations, especially for evolutions within a larger time frame, it is no longer possible to keep all information in the main memory and efficient I/O functionality will be needed.

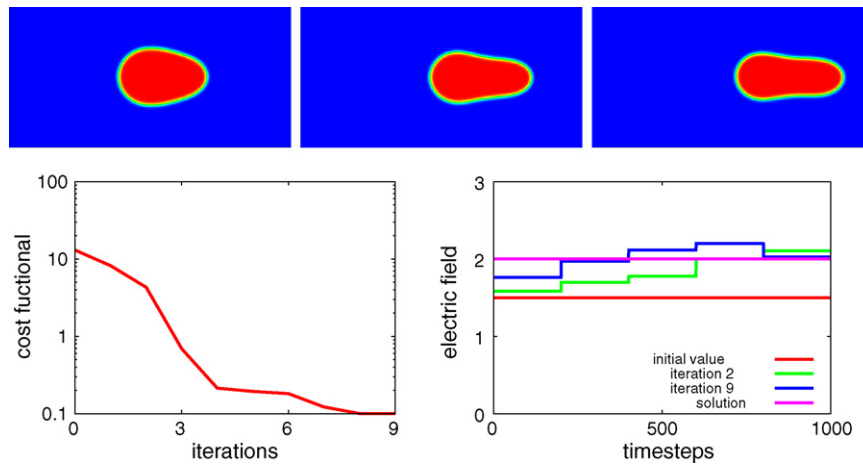


Fig. 6. Computed island position for an ellipse with aspect ratio 1.5 and area πr^2 , $r = 3.0$ at $t = T$ for iteration $k = 0, 2, 9$ (top row—from left to right). Cost functional in logarithmic scale (bottom left) and computed x -component of the electric field (bottom right) for iteration $k = 0, 2, 11$.

5. Conclusions and outlook

Solving an optimal control problem, where the constraint on the states is given by a free boundary problem of 4th order, is a highly non-trivial task. In this article we have presented a first step to solve these types of problems. The formulation of the free boundary problem in terms of a phase-field equation is well suited to formulate an appropriate cost functional and to obtain – using the formal Lagrange approach – corresponding first-order necessary optimality conditions. For some test cases, we were able to demonstrate, that the optimization loop does converge to the expected control. To pass to more interesting examples, an adaptive strategy for mesh refinement/coarsening also for the control problem has to be implemented.

Acknowledgment

This work was supported within SPP 1253 “Optimization with partial differential equations” by DFG through Vo-799/5-1.

References

- [1] E. Bänsch, F. Haußer, O. Lakkis, B. Li, A. Voigt, Finite element method for epitaxial growth with attachment-detachment kinetics, *J. Comput. Phys.* 194 (2004) 409–434.
- [2] J.W. Barrett, H. Garcke, R. Nürnberg, A phase field model for the electromigration of intergranular voids, *Interf. Free Bound.* 9 (2007) 171–210.
- [3] D.N. Bhate, A. Kumar, A.F. Bower, Diffuse interface model for electromigration and stress voiding, *J. Appl. Phys.* 87 (2000) 1712–1721.
- [4] J.W. Cahn, C.M. Elliott, A. Novick-Cohen, The Cahn–Hilliard equation with a concentration dependent mobility: motion by minus the Laplacian of the mean curvature, *Eur. J. Appl. Math.* 7 (1996) 287–301.
- [5] M.R. Gungor, D. Maroudas, Theoretical analysis of electromigration-induced failure of metallic thin films due to transgranular void propagation, *J. Appl. Phys.* 85 (1999) 2233–2246.
- [6] F. Haußer, P. Kuhn, J. Krug, A. Voigt, Morphological stability of electromigration-driven vacancy islands, *Phys. Rev. E* 75 (2007) 046210.
- [7] F. Haußer, A. Voigt, A discrete scheme for parametric anisotropic surface diffusion, *J. Sci. Comput.* 30 (2007) 223–235.
- [8] K.-H. Hoffmann, J. Lishang, Optimal control of a phase field model for solidification, *Numer. Funct. Anal. Optimiz.* 13 (1992) 11–27.
- [9] A. Karma, W.J. Rappel, Quantitative phase-field modeling of dendritic growth in two and three dimensions, *Phys. Rev. E* 57 (1998) 4323–4349.
- [10] P. Kuhn, J. Krug, Islands in a stream, Electromigration-driven shape evolution with crystal anisotropy, in: A. Voigt (Ed.), *Multiscale Modeling in Epitaxial Growth*, Birkhäuser, Basel, 2005, pp. 227–237.
- [11] P. Kuhn, J. Krug, F. Haußer, A. Voigt, Complex shape evolution of electromigration-driven single-layer islands, *Phys. Rev. Lett.* 94 (2005) 166105.
- [12] Y. Liu, K. Oh, J.G. Bai, C.-L. Chang, W. Yeo, J.-H. Chung, K.-H. Lee, W.K. Liu, Manipulation of nanoparticles and biomolecules by electric field and surface tension, *Comput. Methods Appl. Mechan. Eng.* 197 (2008) 2156–2172.
- [13] J. Lowengrub, S. Torabi, A. Voigt, S. Wise, A new phase-field model for strongly anisotropic systems, *Proc. R. Soc. A* 465 (2009) 1337–1359.

- [14] H. Mehl, O. Biham, O. Millo, M. Karimi, Electromigration-induced flow of islands and voids on the Cu(00 1) surface, *Phys. Rev. B* 61 (2000) 4975–4982.
- [15] A. Rätz, A. Ribalta, A. Voigt, Surface evolution of elastically stressed films under deposition by a diffuse interface model, *J. Comput. Phys.* 214 (2006) 187–208.
- [16] O. Pierre-Louis, T.L. Einstein, Electromigration of single-layer clusters, *Phys. Rev. B* 62 (2000) 13697–13706.
- [17] M. Rusanen, P. Kuhn, J. Krug, Kinetic Monte Carlo simulations of oscillatory shape evolution for electromigration-driven islands, *Phys. Rev. B* 74 (2006) 245423.
- [18] M. Schimschak, J. Krug, Electromigration-driven shape evolution of two-dimensional voids, *J. Appl. Phys.* 87 (2000) 695–703.
- [19] J. Sprekels, S. Zheng, Optimal control problems for a thermodynamically consistent model of phasefield type for phase transitions, *Adv. Math. Sci. Appl.* 1 (1992) 113–125.
- [20] K.N. Tu, Recent advances on electromigration in very-large-scale-integration of interconnects, *J. Appl. Phys.* 94 (2003) 5451–5473.
- [21] A. Voigt, S. Vey, AMDiS—adaptive multidimensional simulations, *Comput. Visual. Sci.* 10 (2007) 57–67.